

論文 / 著書情報  
Article / Book Information

Title	Permittivity Enhancement of Mechanically Strained SrTiO MIM Capacitor
Authors	Shin-Ichiro Kuroki, Masayuki Toda, Masaru Umeda, Koji Kotani, Takashi Ito
Citation	ECS Transactions, Vol. 11, No. 3, pp. 293-299
発行日 / Pub. date	2007, 3
DOI	<a href="http://dx.doi.org/10.1149/1.2778672">http://dx.doi.org/10.1149/1.2778672</a>
権利情報 / Copyright	(c) The Electrochemical Society, Inc. 2007. All rights reserved. Except as provided under U.S. copyright law, this work may not be reproduced, resold, distributed, or modified without the express permission of The Electrochemical Society (ECS). The archival version of this work was published in ECS Transactions, Vol. 11, No. 3, pp. 293-299

## Permittivity Enhancement of Mechanically Strained SrTiO<sub>3</sub> MIM Capacitor

Shin-Ichiro Kuroki<sup>1</sup>, Masayuki Toda<sup>2</sup>, Masaru Umeda<sup>3</sup>,  
Koji Kotani<sup>1</sup>, and Takashi Ito<sup>1</sup>

<sup>1</sup>Graduate School of Engineering, Tohoku University,  
6-6-05 Aza-Aoba, Aramaki, Aoba-ku, Sendai, 980-8579 Japan,  
E-mail: kuroki@ecei.tohoku.ac.jp

<sup>2</sup>Department of Chemistry and Chemical Engineering, Yamagata University,  
4-3-16 Jonan Yonezawa, Yamagata, 992-8510, Japan

<sup>3</sup>WACOM R&D CO., LTD., 4-2-6 Nihonbashi-muromachi,  
Chuo-ku, Tokyo, 103-0022, Japan

The possibility of strain engineering on SrTiO<sub>3</sub> high-k insulator was discussed. The tensile strain on SrTiO<sub>3</sub> thin films increased dielectric constant, and as a frequency became higher, the increment of dielectric constant increased. The mechanism of the tensile strain-induced capacitance increase was also discussed. The tensile strain reduced a damping of titanium-oxygen oscillator in SrTiO<sub>3</sub> film, and titanium-oxygen dipole moment was increased.

### Introduction

According to the scaling rule of ULSI miniaturization, dynamic random access memory (DRAM) technologies demand the new high-k materials that have an equivalent-oxide-thickness (EOT) of < 0.5 nm with the high reliabilities. The surveys of DRAM high-k material and deposition processes have been widely carried out. As a candidate of the next DRAM high-k material, titanate perovskite materials have been investigated. Especially in titanate perovskite materials, SrTiO<sub>3</sub> and (Ba, Sr)TiO<sub>3</sub> particularly have been investigated because of its high dielectric constant. For radio frequency integrated circuits (RFICs), the area of the passive RF metal-insulator-metal (MIM) capacitor in a chip relatively grows with the scaling down of the metal-oxide-semiconductor field effect transistors (MOSFETs), and it is necessary to increase the dielectric constant of RF capacitor for smaller RFICs. The SrTiO<sub>3</sub> thin film for a high performance RF MIM capacitor was also investigated [1].

Elastic strain-induced increase of dielectric constant on (Ba, Sr)TiO<sub>3</sub> film doped with Y (Yttrium) was reported [2]. Compressive strain in the (Ba, Sr)TiO<sub>3</sub> film reduced dielectric constant, and Y-doping was applied to suppress the compressive strain and increase dielectric constant. Effect of iron doping of (Ba, Sr)TiO<sub>3</sub> was also reported [3]. Iron ion was substituted for titanium, and dielectric constant was increased. In a different perspective, strain engineering has been a one of the important issues in front end process of CMOS technologies, e.g., strained-induced subband structure engineering in Si MOSFET [4-5]. Mechanically applied uniaxial strain on CMOS circuit was reported [6]. By use of the four-point bending method, surface strain of up to 0.058 % was produced, and enhancement of drain current and circuit performance were shown.

In this work, effect of uniaxial tensile strain applied mechanically on SrTiO<sub>3</sub> thin film was investigated, and we discussed the mechanism of strain-induced dielectric constant enhancement.

## Experiments

Sample preparation and experimental setup were as follows. A  $\text{SrTiO}_3$  thin film was deposited by metal-organic chemical vapor deposition (MOCVD) on a sputter-deposited Pt (200 nm) /  $\text{TiO}_x$  (20 nm) /  $\text{SiO}_2$  (400 nm) / silicon substrate. The precursors of the  $\text{SrTiO}_3$  MOCVD were bis(2,2,6,6-methylethyltetramethyl-3,5-heptanedionato) strontium [ $\text{Sr}(\text{METHD})_2$ ], and methylpentanediol bis(2,2,6,6-tetramethyl-3,5-heptanedionato) titanium [ $\text{Ti}(\text{MPD})(\text{THD})_2$ ] with a solvent of ethylcyclohexane. The  $\text{SrTiO}_3$  film was deposited at a temperature of 525 °C in a MOCVD reactor. The stoichiometry of the  $\text{SrTiO}_3$  film was  $\text{Sr}/\text{Ti} = 50/50$ . The thickness of the  $\text{SrTiO}_3$  film was 100 nm. Pt top electrode with a thickness of 180 nm was deposited on the top  $\text{SrTiO}_3$  film using RF magnetron sputtering with a screen mask of 2 mm in diameter. Crystallinity of the  $\text{SrTiO}_3$  film was measured by out-of-plane, and in-plane x-ray diffraction (XRD). Leakage current and dielectric properties of the  $\text{SrTiO}_3$  film were investigated using Agilent 4156C precision semiconductor parameter analyzer, and Agilent 4284A LCR meter, respectively. Strain apparatus was installed in CASCADE Microtech summit probe station. By use of a strain apparatus in a probe station, precise measurements on electrical properties of the strained  $\text{SrTiO}_3$  film were carried out.

In the capacitance-voltage measurement, the DC bias voltage  $V_{DC}$  on the  $\text{SrTiO}_3$  MIM capacitor was varied from -2.0 V to +2.0 V at 0.05 V interval, corresponding electric field was from -0.2 MV/cm to +0.2 MV/cm, and the amplitude  $V_{osc}$  of signal voltage was fixed to 0.5 V, and the frequencies  $\omega/2\pi$  of signal voltage were 30, 100, 300, and 500 kHz. The total applied voltage on the  $\text{SrTiO}_3$  MIM capacitor was  $V_{DC} + V_{osc} e^{i\omega t}$ .

### Characteristics of MOCVD $\text{SrTiO}_3$ thin films

The crystallinity of the  $\text{SrTiO}_3$  thin film was measured by out-of-plane, and in-plane XRD. Figure 1 shows the results of XRD measurement. In the out-of-plane XRD spectrum, the strong peak of  $\text{SrTiO}_3$  (200) at 2theta of 46.45 ° was observed, on the other hand, in the in-plane XRD spectrum, the peak of  $\text{SrTiO}_3$  (110) at 2theta of 32.33 ° was dominantly observed. These results showed that the  $\text{SrTiO}_3$  thin film had a crystallinity of (100) in the depth direction of the film, and also had a uniform crystallinity in the surface

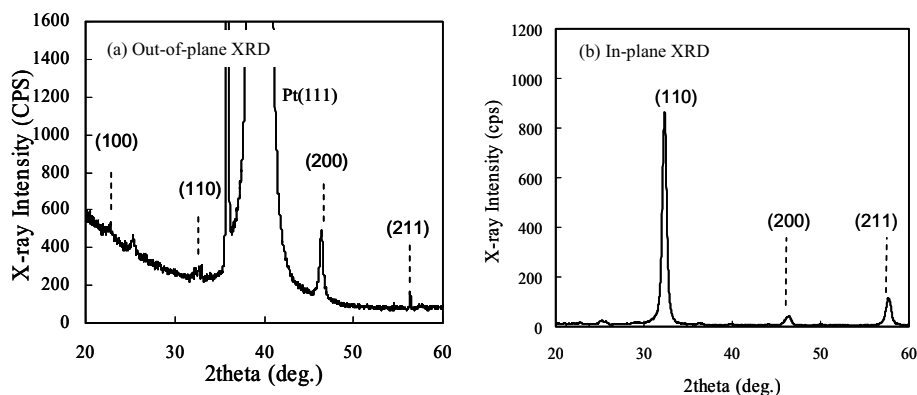


Figure 1. X-ray diffraction pattern of the  $\text{SrTiO}_3$  thin films: (a) out-of-plane measurement and (b) in-plane measurement.

direction, for example, in this measurement, the (110) peak was observed. In the in-plane XRD spectrum, the (200) peak was observed at a 2theta of 46.42 °, corresponding lattice distance was 0.1065 nm, on the other hand, in the out-of-plane XRD measurement, the (200) peak was observed at a 2theta of 46.45 °, corresponding lattice distance was 0.1064 nm. These results showed that the lattice distance of surface direction was slightly longer than that of depth direction.

The leakage current density of SrTiO<sub>3</sub> MIM capacitor was  $1.51 \times 10^{-6}$  and  $2.77 \times 10^{-6}$  A/cm<sup>2</sup> at bias electric fields of +0.10 and +0.20 MV/cm, respectively. This result showed that the MOCVD SrTiO<sub>3</sub> film had a good performance for DRAM high-k insulator.

### Tensile Strain on SrTiO<sub>3</sub> MIM capacitor

Figure 2 shows a schematic diagram of the two-point bending method. The sample wafer with the SrTiO<sub>3</sub> film was installed on the bending apparatus and uniaxial tensile stress was mechanically applied, and the surface strain was produced on the SrTiO<sub>3</sub> film. Here the surface strain was estimated by the equation:

$$\zeta = \frac{\Delta L}{L} \bigg|_{\text{Surface}} \cong \frac{T \cdot \Delta y}{L^2}, \quad [1]$$

where  $T$  is a thickness of silicon substrate, and  $L$  is a length of sample from supporting point of substrate mounting, to the point that is strain forced, and  $\Delta y$  is a displacement of the strained-forced point of silicon substrate. This surface strain  $\zeta$  corresponding to the elastic strain tensor  $e_{ij}$  is a diagonal element  $e_{xx}$ , and the elastic strain tensor is defined by the equation  $e_{ij} = (\partial_i u_j + \partial_j u_i) / 2$ , where  $u_i$  is a displacement of a position  $x_i$ :  $x_i \rightarrow x_i + u_i$ .

The results of capacitance-voltage measurements were summarized in Fig. 3. In this figure, the capacitance axis was converted to dielectric constant. The value of dielectric constants in Fig. 3 was average value from -2.0 V to +2.0 V in each measurement. At a low frequency of 30 kHz, after tensile strain was applied, the dielectric constant remained at a same value. At a high frequency of applied voltage, the effect of the tensile strain

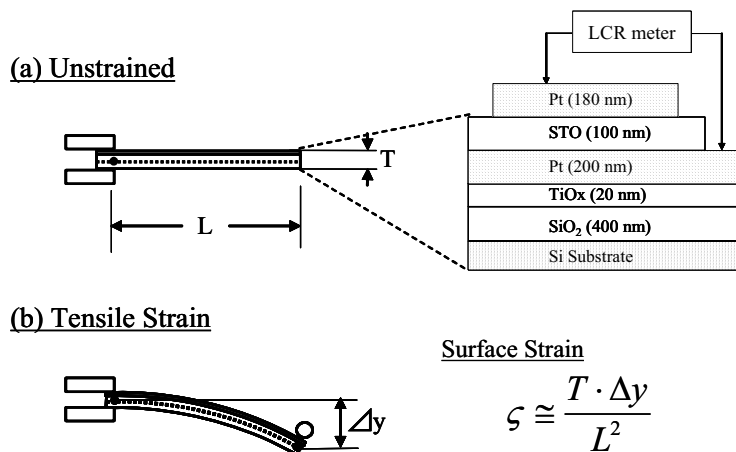


Figure 2. Schematic diagram of two-point bending method used for applying uniaxial tensile strain on the SrTiO<sub>3</sub> thin films.

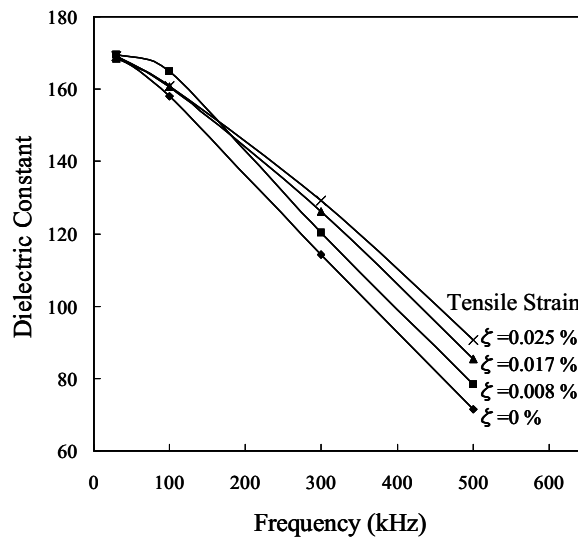


Figure 3. Tensile strain effect on dielectric constant of the SrTiO<sub>3</sub> thin films. After the tensile strain forced, the dielectric constant became larger.

appeared, and dielectric constant was increased. At a frequency of 500 kHz, the dielectric constant of the unstrained SrTiO<sub>3</sub> was 71.49, while after the tensile strain forced, and the dielectric constant became larger and was 90.66. As the frequency was increased, the dielectric constant became smaller. At a frequency of 30 kHz, the unstrained SrTiO<sub>3</sub> thin film had a dielectric constant of 169.38, and at 500 kHz it became 71.49.

### Tensile Strain and Ion Dynamics

Here, we discussed the effect of the tensile strain on SrTiO<sub>3</sub>, especially the relation between the strain and ion dynamics. In SrTiO<sub>3</sub> film, titanium ion and oxygen ion form ionic dipole moment, and contribute to high dielectric constant. The schematic diagram of the titanium-oxygen dipole moment is shown in Fig. 4 (a). When external electric field is applied to SrTiO<sub>3</sub> film, titanium ion moves and oscillates against oxygen ion plane. This dynamics is represented by a simple harmonic oscillator under external electric field as shown in Fig. 4 (b). Titanium ion and oxygen ion plane has a harmonic interaction with a relative distance  $z$ , the equation of motion is given by the equation:

$$M_{ion} \frac{d^2 z}{dt^2} + 2M_{ion} \Gamma \frac{dz}{dt} + M_{ion} \omega_0^2 z = Z_{ion} e E_0 \exp(i\omega t), \quad [2]$$

where  $M_{ion}$  is an ion mass,  $\Gamma$  is a damping coefficient,  $\omega_0$  and  $Z_{ion}$  are eigenfrequency and valence of ion, respectively. After solving this equation, the polarization  $P = Z_{ion} e N_{ion} z$  is obtained, and the dielectric constant is derived as

$$\varepsilon = 1 + \frac{e^2 Z_{ion}^2 N_{ion}}{\varepsilon_0 M_{ion}} \frac{1}{(\omega_0^2 - \omega^2) + i2\Gamma\omega}, \quad [3]$$

and the real part of dielectric constant is given by the equation:

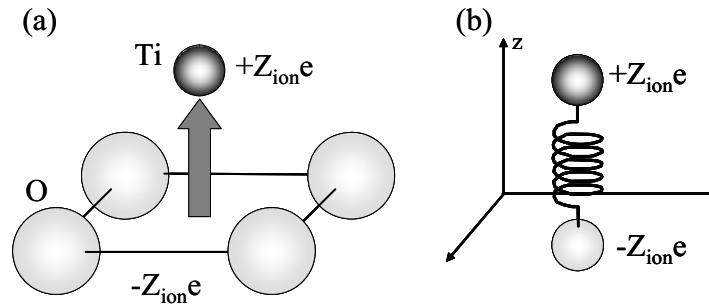


Figure 4. Schematic diagram of titanium-oxygen polarization in the SrTiO<sub>3</sub> thin films: (a) polarized titanium-oxygen configuration in the SrTiO<sub>3</sub> perovskite structure, and (b) the corresponding harmonic oscillator.

$$\frac{1}{k-1} = C^{-1} \frac{(\omega_0^2 - \omega^2)^2 + 4\Gamma^2 \omega^2}{\omega_0^2 - \omega^2}, \quad [4]$$

where  $k$  is the real part of the dielectric constant  $\varepsilon$ , and  $C$  is a constant coefficient  $C = (e^2 Z_{ion}^2 N_{ion}) / (\varepsilon_0 M_{ion})$ . These equations represent the dielectric dispersion relation induced by ionic polarization. At neighbor of an arbitrary frequency  $\omega'$ , the dielectric dispersion equation is approximately given by the parabolic equation,

$$\frac{1}{k-1} \Big|_{\omega' \sim \text{Neighbor}} = \frac{\omega_0^2}{C} \left[ \left( \frac{4 \frac{\Gamma^2}{\omega_0^2}}{\left(1 - \frac{\omega'^2}{\omega_0^2}\right)^2} - 1 \right) \frac{\omega^2}{\omega_0^2} + \left( 1 - \frac{4 \frac{\Gamma^2}{\omega_0^2} \cdot \left(\frac{\omega'^2}{\omega_0^2}\right)^2}{\left(1 - \frac{\omega'^2}{\omega_0^2}\right)^2} \right) \right], \quad [5]$$

especially at the infrared limit  $\omega' / \omega_0 \rightarrow 0$ , the dielectric dispersion relation becomes the simple parabolic equation as:

$$\frac{1}{k-1} \Big|_{\text{Infrared limit: } \omega' / \omega_0 \rightarrow 0} = \frac{\omega_0^2}{C} \left[ \left( 4 \frac{\Gamma^2}{\omega_0^2} - 1 \right) \frac{\omega^2}{\omega_0^2} + 1 \right]. \quad [6]$$

At the infrared limit, the damping coefficient  $\Gamma$  appears only in slope of  $\omega^2 / \omega_0^2$ .

Figure 5 shows the  $1/(k-1) - (\omega/2\pi)^2$  plot of the strained SrTiO<sub>3</sub> films. It was found that each curve was linear to  $\omega^2$ , and have a almost same y-intercept. The slope of the linear curves decreased as the tensile strain applied on SrTiO<sub>3</sub> films. These results show the dispersion relation at the infrared limit is proper approximation at the frequency region of 30 - 500 kHz. Based on the infrared-limit picture, invariable y-intercept showed that the tensile strain did not affect the eigenfrequency  $\omega_0$  of titanium-oxygen harmonic oscillation, and the decrease of the curve's slope showed that the strain affects the damping coefficient of titanium-oxygen ion dynamics. Figure 6 shows the damping coefficient as a function of tensile strain. It was found that as the tensile strain was applied to the SrTiO<sub>3</sub> film, the damping coefficient decreased. The reduction of the damping coefficient increased the electric dipole moment in the titanium-oxygen ionic oscillator, and the dielectric constant of the SrTiO<sub>3</sub> film was increased. From another point of view, the reduction of the damping coefficient was considered as a result of

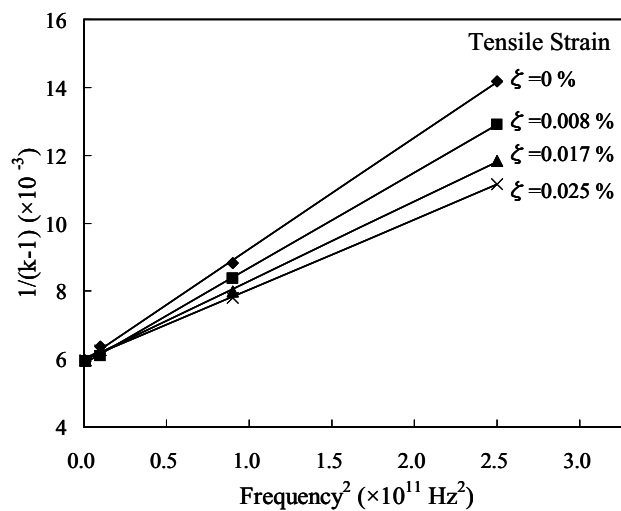


Figure 5.  $1/(k-1)$ -frequency relation:  $1/(k-1)$  increased linearly as a function of  $(\omega/2\pi)^2$ .

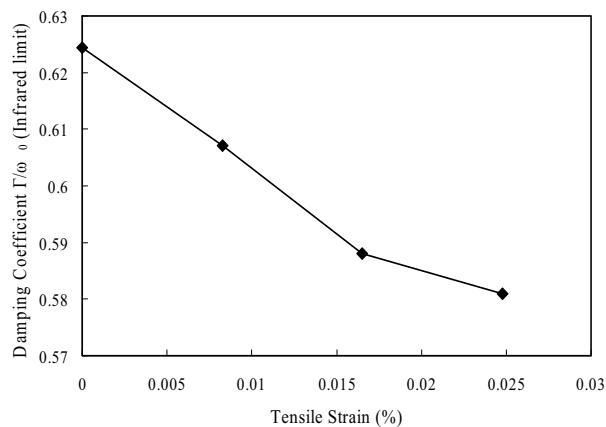


Figure 6. Damping coefficient as a function of tensile strain. The damping coefficient was normalized by the eigenfrequency of ionic titanium-oxygen oscillator.

energy dissipation reduction; the energy dissipation via crystal lattice oscillation, in other word, phonon conduction decreased by applying the tensile strain.

### Deep Tensile Strain and Dielectric Property

Figure 7 shows the increase of the dielectric constant induced by deep tensile strain. Up to the tensile strain of 0.025 %, at frequencies of 300 and 500 Hz, dielectric constants were increased linearly, and above the tensile strain of 0.025 %, increase of dielectric constant was saturated. This result showed the threshold of the strain-induced capacitance increase was situated near the tensile strain of 0.025 %.

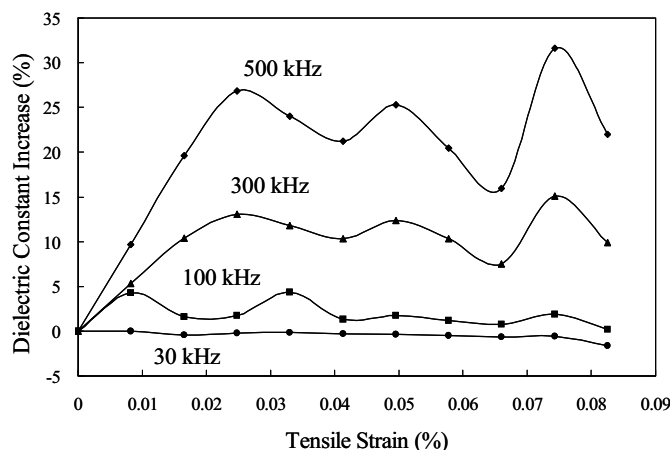


Figure 7. Dielectric constant increase as a function of tensile strain.

### Summary

The mechanically applied uniaxial strain on the  $\text{SrTiO}_3$  MIM capacitor was investigated. The dielectric constant was enhanced by the uniaxial tensile strain, and at a frequency of 500 kHz, enhancement of 26.8 % was achieved. The effect of the tensile strain on  $\text{SrTiO}_3$  ion dynamics was discussed. The tensile strain decreased the damping coefficient of titanium-oxygen ion oscillator. The reduction of the damping coefficient increased the electric dipole moment, and as a result, the dielectric constant of the  $\text{SrTiO}_3$  film was increased. The threshold strain of the tensile strain-induce capacitance increase was 0.025 %. Under the threshold of 0.025 %, dielectric constant increased linearly, and above the threshold, dielectric constant was saturated. These results indicate the importance of strain design in fabrication process of high-k capacitors.

### Acknowledgments

A part of this work was supported by Special Coordination Fund for Promoting Science and Technology of Ministry of Education, Culture, Sports, Science and Technology (MEXT).

### References

1. C. C. Huang, K. C. Chiang, H. L. Kao, A. Chin, and W. J. Chen, IEEE Microw. Wireless Compon. Lett., **16**, 493 (2006).
2. R. Wang, P. C. McIntyre, J. D. Baniecki, K. Nomura, T. Shioga, K. Kurihara, and M. Ishii, Appl. Phys. Lett., **87**, 192906 (2005).
3. K. Imai, S. Takeno, and K. Nakamura, Jpn. J. Appl. Phys., **41**, 6060 (2002).
4. S. Takagi, J. Koga, A. Toriumi, Technical Digest of International Electron Devices Meeting 1997 (IEDM 1997), 219 (1997).
5. T. Miyashita, A. Hatada, Y. Shimamune, T. Owada, N. Tamura, T. Aoyama, and S. Sato, Jpn. J. Appl. Phys., **46**, 2084 (2007).
6. T. Miyashita and T. Tanaka, Extended Abstract of the 2005 Int. Conf. on Solid State Devices and Materials, 40 (2005).